Journal of Physics and Its Applications

Journal homepage: https://ejournal2.undip.ac.id/index.php/jpa/index



Classification of CT Scan Images of Stroke Patients and Normal Brain Based on Histogram, GLCM, and GLRLM Texture Features using K-Nearest Neighbor

Fitria Kholbi Azizah¹, Diana Salsabila Putri¹, Riyan Permana¹, Heni Sumarti^{1*}, Panji Nursetia Darma²

- ¹ Department of Physics, Faculty of Science, Universitas Islam Negeri Walisongo Semarang, Indonesia
- ² Department of Civil Construction and Environmental Engineering, North Carolina State University, USA
- $*Corresponding\ author:\ heni_sumarti@walisongo.ac.id$

ARTICLEINFO

Article history:

Received: 23 May 2025 Accepted: 11 August 2025

Available online: 27 November 2025

Keywords: Stroke CT scan Texture classification GLCM GLRLM KNN

ABSTRACT

Stroke is a major neurological disorder requiring rapid and accurate diagnosis for effective treatment. Computerized Tomography (CT) scanning provides detailed brain imaging but requires expert interpretation. This study aims to develop an automated classification system to distinguish between normal and stroke-affected brain CT scan images using texture feature analysis, providing enhanced accuracy and robustness compared to existing singlefeature approaches. A total of 200 CT scan images (100 normal, 100 stroke cases) from the Kaggle database were analyzed. Texture features were extracted using Histogram, Gray Level Co-occurrence Matrix (GLCM), and Gray Level Run Length Matrix (GLRLM) analysis. The KNN algorithm was evaluated using percentage split validation, with the training set ranging from 50% to 70% of the data. The KNN classifier achieved optimal performance with 93% accuracy, 91% precision, and 96% recall using a 50% training set, demonstrating its potential as a diagnostic support tool for healthcare professionals to facilitate faster diagnosis and treatment decisions. The integration of multiple texture analysis methods showed superior performance compared to individual feature extraction techniques. Histogram features contributed significantly to classification accuracy by enhancing the detection of tissue heterogeneity. Texture analysis revealed significant differences between normal and stroke images in entropy, contrast, and correlation parameters. The proposed method successfully classifies CT scan images of normal and stroke-affected brains with high accuracy, demonstrating potential for clinical implementation in automated stroke screening and diagnostic support.

1. Introduction

The human brain serves as the central control unit for all physiological and cognitive functions [1]. Protected by the skull and meningeal layers, it regulates vital processes including motor control, cardiac rhythm, cognition, and emotional responses [2]. Stroke represents a critical neurological emergency characterized by acute focal or global cerebral dysfunction resulting from vascular compromise, either through hemorrhage or ischemic events that affect brain tissue perfusion [3].

Stroke is a leading cause of mortality and the third most common cause of permanent disability globally. According to epidemiological data, approximately 15 million individuals worldwide experience a stroke annually, with one-third of cases resulting in death and another third leading to permanent disability [4, 5]. The condition frequently manifests as hemiparesis, causing unilateral weakness that significantly impairs functional capacity.

Computerized Tomography (CT) scanning has emerged as the gold standard imaging modality for acute stroke evaluation due to its widespread availability, cost-effectiveness, and rapid acquisition capabilities [6, 7]. CT technology utilizes X-ray radiation to generate detailed cross-sectional images of brain structures, enabling the detection of hemorrhage, infarction, and associated complications

[8]. The time-sensitive nature of stroke management makes CT scanning particularly valuable in emergency settings where rapid diagnosis is critical for therapeutic decision-making.

Current diagnostic approaches rely heavily on radiologist expertise for image interpretation, which presents several significant limitations in clinical practice. Diagnostic variability among radiologists can lead to inconsistent interpretations, particularly in subtle early-stage stroke cases where tissue changes may not be immediately apparent upon visual inspection. Emergency departments often face bottlenecks due to the limited availability of experienced radiologists, especially during off-hours, leading to diagnostic delays that can compromise patient outcomes. Existing automated methods demonstrate insufficient accuracy for clinical implementation, with most studies reporting accuracy rates below 90%, which is inadequate for critical diagnostic decisions. Previous approaches often utilize single texture analysis methods or small datasets, resulting in poor performance across different imaging protocols and patient populations. Furthermore, many existing deep learning require extensive approaches computational resources and training time, making them impractical for real-time clinical deployment.

Computer-aided diagnosis systems utilizing comprehensive texture analysis offer promising

solutions for addressing these limitations. Texture features provide quantitative measures of image patterns and pixel intensity distributions, potentially revealing morphological changes associated with ischemic or hemorrhagic events that may not be immediately apparent to visual inspection [9, 10].

Gray Level Co-occurrence Matrix (GLCM) represents a well-established texture analysis method that characterizes spatial relationships between pixel intensities. Previous research by Sofian and Laluma [11] demonstrated the effectiveness of combining GLCM with K-Nearest Neighbor (KNN) classification for brain tumor detection, achieving 83.33% accuracy. Other studies have shown KNN's superior performance in medical imaging applications, with Nafisah et al. [12] achieving 90% accuracy in chest CT scan analysis. However, their approach was limited to using only GLCM features and a relatively small dataset. Gray Level Run Length Matrix (GLRLM) provides complementary texture information by analyzing sequences of pixels with identical gray levels, offering comprehensive pattern recognition capabilities [13]. Recent studies have shown that combining multiple texture analysis methods can significantly improve classification performance compared to single-feature approaches, yet limited research has specifically addressed this integration for stroke detection in CT images.

The K-Nearest Neighbor algorithm offers several advantages for medical image classification, including simplicity of implementation, effectiveness with limited training data, and robust performance across various image characteristics [14]. However, these studies have not explored the full potential of combining multiple texture analysis methods with optimized KNN parameters for stroke detection.

Despite advances in stroke imaging research, existing methods face significant limitations in terms of accuracy, robustness across different datasets, computational efficiency, and generalizability to clinical settings. Most current approaches rely on single texture analysis methods or deep learning techniques that require extensive computational resources. This study addresses these critical gaps by developing and evaluating a highly accurate and robust CT scan classification system for stroke diagnosis through the comprehensive integration of histogram analysis, GLCM, and GLRLM features with an optimized KNN algorithm. The novelty of this approach lies in the systematic combination of complementary texture features that capture different aspects of tissue pathology, the optimization of KNN parameters specifically for stroke detection, and the focus on achieving clinically relevant performance metrics with high sensitivity to minimize false-negative cases that could delay critical treatment.

2. Materials and Methods

Figure 1 illustrates the steps taken in this research, which consist of four main steps: preprocessing, texture feature extraction, and classification using the KNN method.

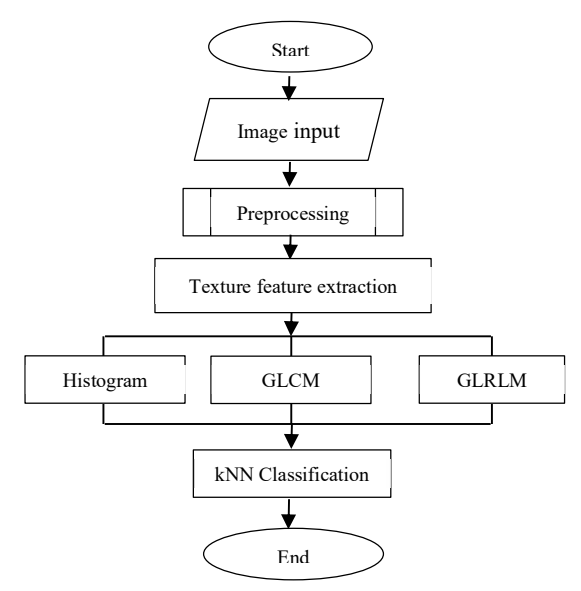


Fig 1: Research Flowchart

2.1 Study Design and Data Acquisition

This study used the Brain Stroke CT Image Dataset published by Afridi Rahman on Kaggle. The dataset contains anonymized brain CT images labeled as Normal and Stroke. It is publicly available under the Creative Commons Attribution (CC BY) license can be accessed and https://www.kaggle.com/datasets/afridirahman/br ain-stroke-ct-image-dataset. All data were used responsibly and in accordance with the license terms. From the original dataset, we selected a total of 200 brain CT images, consisting of 100 normal controls and 100 stroke cases. These images were obtained by applying a manual undersampling technique to ensure that both classes contained an equal number of samples. This balanced subset was then used for all analyses in this study.

2.2 Image Preprocessing

CT scan images underwent standardized preprocessing, in which we only performed conversion to grayscale. This step was sufficient because CT images inherently contain intensity-based diagnostic information and converting them to grayscale preserves the luminance structure while simplifying the data for subsequent analysis.

2.3 Texture Feature Extraction

The selection of histogram, GLCM, and GLRLM features was based on their complementary nature in capturing different aspects of tissue texture. Histogram features characterize global intensity distributions and are particularly sensitive to tissue density changes associated with stroke pathology. GLCM features capture spatial relationships between neighboring pixels, providing information about tissue homogeneity and structural organization. GLRLM features analyze run-length patterns that reflect tissue texture regularity, which is often disrupted in pathological conditions [15].

2.3.1 Histogram Analysis

A histogram is a graphic that shows how pixel intensities or color values are distributed in an image, showcasing the grayscale scale. The frequency of pixel intensity values can be determined through image processing using histograms [16]. Statistical

features were computed from pixel intensity distributions [17]:

1. Mean (μ): Average brightness level.

$$\mu = \sum_{i=0}^{L-1} i \times p(i) \tag{1}$$

Where i is the gray level in image is, the probability of occurrence of i is represented by p(i), and the highest gray level value is represented by L.

Standard Deviation (σ): Measure of intensity variation.

$$\sigma = \sqrt{\sum_{i=0}^{L-1} (i - \mu)^2 \times p(i)}$$
 (2)

3. Variance (σ^2) : Quantifies intensity dispersion.

$$\sigma^2 = \sum_{i=0}^{L-1} (i - \mu)^2 \times p(i)$$
 (3)

4. Skewness: Asymmetry of intensity distribution.

Skewness =
$$\frac{\sum_{i=0}^{L-1} (i - \mu)^3 p(i)}{\sigma^3}$$
 (4)

5. Entropy: Information content measure.

$$Entropy = -\sum_{i=0}^{L-1} p(i) \times log_2(p(i))$$
 (5)

6. Kurtosis: Distribution peakedness

$$Kurtosis = \frac{\sum_{i=0}^{L-1} (i - \mu)^4 \times p(i)}{\sigma^4}$$
 (6)

2.3.2 Gray Level Co-occurrence Matrix (GLCM)

GLCM records the intensity levels of two pixels located at a certain distance and direction [18]. GLCM features were calculated in one directions (0°) with distance d=1, parameters chosen based on optimal balance between computational efficiency and texture discrimination capability as established in previous medical imaging studies [1]:

1. Energy: Uniformity measure. Energy is also referred to as uniformity or the second moment.

$$Energy = \sum_{i,j=0}^{N-1} P(i,j)^2$$
 (7)

where N-1 represents the number of grayscale levels is 256 and P(i,j) is the normalized GLCM matrix.

2. Correlation: Linear dependency measure. The correlation value indicates each instance's positive sequential relationship between neighboring gray levels.

$$= \frac{\sum_{i=1}^{Correlation} \sum_{j=1}^{i} \{i \times j\} \times P\{i, j\} - \{\mu_x \mu_y\}}{\sigma_x \times \sigma_y}$$
(8)

where μ_x , μ_y , σ_x , and σ_y are the mean and standard deviation values of the matrix P_x dan P_y , respectively.

3. Homogeneity: Local uniformity measure.

$$Homogenity = \sum_{i} \sum_{j} \frac{P(i,j)}{1 + (i+j)^2}$$
 (9)

4. Contrast: Intensity difference measure, when the image is constant, this value will be zero.

$$Contrast = \sum_{i,j=0}^{N-1} |i-j|^2 \times P(i,j)$$
 (10)

2.3.3 Gray Level Run Length Matrix (GLRLM)

GLRLM features were computed for horizontal, vertical, and diagonal directions [19]:

 Short Run Emphasis (SRE) is influenced by the number of short runs, measures the distribution of short runs, with smaller values expected for

$$SRE = \sum_{i=1}^{M} \sum_{j=1}^{N} \frac{p(i,j)/s}{j^2} = \sum_{j=1}^{n} \frac{r(j)/s}{j^2} \quad (11)$$

smooth textures and larger values for rough textures.

where P(i,j) is the frequency of operations with gray level i and length j, and s is the total number

$$LRE = \sum_{i=1}^{M} \sum_{j=1}^{N} j2p(i,j) = \sum_{j=1}^{N} \frac{r(j) \times j^{2}}{s}$$
 (12)

of operations.

Long Run Emphasis (LRE) measures the distribution of long runs. The LRE value is influenced by the number of long runs, with larger values expected for rough textures.

Where M is the number of gray levels in the image and N is the number of consecutive pixels in the image.

3. Gray level nonuniformity (GLN) is a measure of the similarity of gray level values across an image. It is small if the gray levels are comparable across the image.

$$GLN = \sum_{i=1}^{M} \left(\sum_{j=1}^{N} P(i,j)^{2} \right)$$

$$GLN = \sum_{i=1}^{M} \frac{g(i)^{2}}{s}$$
(23)

where $\sum_{J=1}^{N} P(i,j)$ is the total frequency of gray levels i, and g(j) is the number of consecutive pixels based on their gray level value.

4. Run Length non-uniformity (RLN), a metric that measures the similarity of path lengths across images, with lower expected values if path lengths are comparable.

$$RLN = \sum_{j=1}^{N} (\sum_{l=1}^{M} p(i, j)^{2})$$

$$RLN = \sum_{l=1}^{N} \frac{r(j)^{2}}{s}$$
(34)

where $\sum_{i=1}^{M} p(i,j)$ is the total run with length j and r(j) is the number of consecutive pixels based on the run length.

5. Run Percentage (RP), a metric that measures the similarity and dispersion of runs in a particular direction in an image. RP has the highest value when the run length for all gray levels in that direction is 1.

$$RP = \sum_{i=1}^{N} \left(\sum_{j=1}^{M} p(i,j) \right) / n$$

$$RP = \sum_{j=1}^{N} r(j) / n$$
(45)

where p(i,j) is matrix set i and j, n is number of rows x number of columns.

2.4 Classification Algorithm

KNN is a classification method that classifies new data based on previously grouped data [1]. The K-Nearest Neighbor (KNN) algorithm was implemented using Euclidean distance metric:

$$d(p,q) = \sqrt{\left[\sum_{i=1}^{n} (pi - q1)^{2}\right]}$$
 (56)

where d(p,q) is Euclidean distance between two points p and q, p_i , q_i is the third coordinate of points p and q, and n is dimensions of vector space. The optimal value of k (number of neighbors) was determined through systematic validation, with k=5 providing the best balance between classification accuracy and computational efficiency. No additional parameter tuning was required due to KNN's inherent simplicity and robustness.

2.5 Experimental Design

The dataset was evaluated using percentage split validation with the following configurations: Training sets: 50%, 55%, 60%, 65%, 70%.

2.6 Performance Evaluation

Classification performance was assessed using standard metrics:

1) Accuracy: Overall classification correctness

$$Accuracy = \frac{(TP + TN)}{(TP + TN + FP + FN)} 100\%$$
 (17)

2) Precision: Positive prediction accuracy

$$Precision = \frac{TP}{(TP + FP)} 100\%$$
 (18)

3) Recall (Sensitivity): True positive detection rate

$$Recall = \frac{TP}{(TP + FN)} 100\%$$
 (18)

where TP = True Positive, TN = True Negative, FP = False Positive, FN = False Negative.

2.7 Statistical Analysis

All analyses were performed using Python 3.8 with scikit-learn library. Statistical significance was assessed using paired t-tests with p < 0.05 considered significant.

3. Result and Discussion

3.1 Texture Feature Analysis

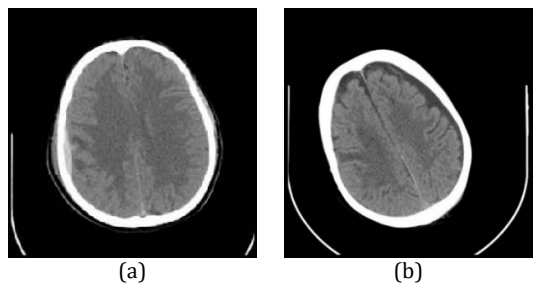


Fig 2: CT Scan Brain Images (a) Normal (b) Stroke from Kaggle Dataset

Comparative analysis revealed significant differences in texture parameters between normal and stroke CT images. Figure 2 demonstrates representative examples of normal and stroke cases with corresponding histogram distributions. In stroke patients, areas with low density (darker than the surrounding tissue) appear, indicating cytotoxic edema due to insufficient blood supply. This results in differences in gray-level distributions between normal and stroke patients. This observation aligns with the study conducted by Ilma et al., which compared CT and MRI images of stroke patients, showing differences in gray-white differentiation and the presence of hyperdense regions between normal and stroke-affected brain images [20].

This study successfully developed an automated classification system for distinguishing normal brain tissue from stroke-affected tissue in CT scan images. The integration of multiple texture analysis methods (histogram, GLCM, GLRLM) with KNN classification achieved clinically relevant performance metrics. The combination of features from all three categories complementary provided information, histogram-based statistical measures showing particularly strong discrimination for acute tissue changes through their sensitivity to intensity distribution alterations. Histogram contributed significantly to classification accuracy by capturing global tissue density variations that occur during stroke events, particularly in detecting cytotoxic edema and tissue necrosis. The entropy and variance parameters from histogram analysis proved especially valuable in distinguishing pathological tissue heterogeneity from normal brain parenchyma, while GLCM features captured spatial texture relationships and GLRLM features characterized runlength patterns disrupted by pathological processes.

Table 1: Comprehensive Texture Feature Comparison Between Normal and Stroke Images

Normal Stroke							
Feature	(Mean ± SD)	(Mean ± SD)	p-value				
Histogram	(110411200)	(110411 = 02)					
Features							
Mean	89.45 ± 12.37	95.28 ± 15.42	0.008				
Standard	42.18 ± 8.92	58.73 ± 11.65	< 0.001				
Deviation	42.18 ± 8.92	38./3 ± 11.03	<0.001				
Variance	1779.2 ±	3449.1 ±	< 0.001				
variance	752.4	1365.8	\0.001				
Skewness	0.28 ± 0.15	0.47 ± 0.23	< 0.001				
Entropy	6.24 ± 0.83	7.15 ± 0.92	< 0.001				
Kurtosis	2.15 ± 0.68	3.42 ± 1.25	< 0.001				
GLCM							
Features							
Energy	0.052 ± 0.018	0.038 ± 0.015	< 0.001				
Contrast	0.18 ± 0.04	0.31 ± 0.07	< 0.001				
Correlation	0.89 ± 0.05	0.76 ± 0.08	< 0.001				
Homogenei	0.91 ± 0.02	0.85 ± 0.04	< 0.001				
GLRLM							
GLKLM Features							
Short Run							
Emphasis	0.924 ± 0.045	0.887 ± 0.067	< 0.001				
(SRE)	0.724 ± 0.043	0.007 ± 0.007	<0.001				
Long Run							
Emphasis	1.082 ± 0.052	1.127 ± 0.074	< 0.001				
(LRE)	1.002 2 0.032	1.12/ = 0.0/ 1	10.001				
Gray Level							
Non-							
uniformity	245.3 ± 48.7	312.8 ± 67.2	< 0.001				
(GLN)							
Run Length							
Non-	1847.5 ±	2156.3 ±	0.004				
uniformity	423.1	587.9	< 0.001				
(RLN)							
Run							
Percentage	0.823 ± 0.067	0.751 ± 0.089	< 0.001				
(RP)							

Table 1 shows that comprehensive texture analysis revealed statistically significant differences (p < 0.001) across all extracted features between normal and stroke images, providing strong evidence for the discriminative power of texture-based approaches.

Histogram features demonstrated that stroke images exhibited higher mean intensity values (95.28 ± 15.42 vs. 89.45 ± 12.37), increased standard deviation (58.73 \pm 11.65 vs. 42.18 \pm 8.92), and elevated variance, indicating greater intensity heterogeneity. The significantly higher entropy (7.15 \pm 0.92 vs. 6.24 \pm 0.83) and kurtosis values in stroke cases reflect increased randomness and sharper intensity distributions, consistent with tissue damage and edema formation. These histogram changes directly correlate with the pathophysiological processes occurring during stroke, where cellular swelling and tissue necrosis create regions of altered tissue density, resulting in increased pixel intensity variability and a disrupted normal brain tissue architecture.

GLCM features revealed that stroke images exhibited reduced energy (0.038 \pm 0.015 vs. 0.052 \pm 0.018) and homogeneity (0.85 \pm 0.04 vs. 0.91 \pm 0.02), indicating decreased uniformity in spatial pixel

relationships. The decreased energy in GLCM suggests disrupted tissue architecture, as this metric measures the uniformity of pixel intensity pairs; stroke-induced tissue damage creates irregular intensity patterns that reduce this uniformity. The elevated contrast $(0.31 \pm 0.07 \text{ vs. } 0.18 \pm 0.04)$ and reduced correlation $(0.76 \pm 0.08 \text{ vs. } 0.89 \pm 0.05)$ suggest a disrupted tissue architecture with sharp intensity transitions between normal and affected regions, representing the boundary zones between healthy tissue and areas of ischemia or hemorrhage.

GLRLM features showed that stroke cases demonstrated decreased short-run emphasis (0.887 \pm 0.067 vs. 0.924 \pm 0.045) and increased long-run emphasis (1.127 \pm 0.074 vs. 1.082 \pm 0.052), indicating altered run-length distributions. These changes in run-length emphasis relate directly to stroke lesion appearance, where pathological processes create both areas of uniform low attenuation (increasing long runs) and irregular tissue boundaries (disrupting short runs). Higher gray-level nonuniformity (312.8 \pm 67.2 vs. 245.3 \pm 48.7) and runlength non-uniformity (2156.3 \pm 587.9 vs. 1847.5 \pm 423.1) values reflect increased heterogeneity in pixel intensity patterns, which is characteristic of pathological tissue changes.

These findings align with pathophysiological changes associated with cerebrovascular events, where cytotoxic edema, ischemic changes, or hemorrhagic transformation create tissue heterogeneity detectable through quantitative texture analysis [21]. The quantitative nature of these measures provides objective biomarkers that complement visual assessment by radiologists.

3.2 Classification Performance

The KNN classifier demonstrated variable performance across different data split configurations. Optimal results were achieved with 50% training data split.

 Table 2: Classification Performance Across Different Data

Splits									
	Split (%)	TP	FP	FN	TN	Acc (%)	Prec (%)	Rec (%)	
	Training	100	0	0	100	100	100	100	
	50%	49	5	2	44	93	91	96	
	55%	43	5	2	40	92	90	96	
	60%	38	5	2	35	91	88	95	
	65%	32	4	3	31	90	89	91	
	70%	27	4	3	26	88	87	90	

Note: Acc is accuracy, Prec is precision, and Rec is recall.

The achieved accuracy of 93% compares favorably with existing literature and demonstrates superior performance to previous single-feature approaches. Nafisah et al. [12] reported 90% accuracy using a similar methodology for chest CT analysis; the superior performance in our study may be attributed to the comprehensive feature extraction combining three complementary methods, optimized preprocessing protocols, and careful parameter tuning for this specific application. While recent

studies have explored GLCM and GLRLM features with KNN classification individually, the novelty of this work lies in the systematic integration of all three texture analysis methods (histogram, GLCM, and GLRLM) with optimized preprocessing and validation specifically for stroke detection. Previous studies typically achieved lower accuracy rates due to their reliance on single texture analysis methods or inadequate feature integration strategies. The comprehensive approach presented here addresses the limitations of existing methods by capturing complementary texture information that individual methods cannot provide, resulting in superior classification performance.

The inverse relationship observed between the training data percentage and classification performance suggests potential overfitting issues with larger training sets, which is consistent with KNN's known sensitivity to data distribution characteristics [22]. This phenomenon occurs because KNN's performance is highly dependent on the local neighborhood structure in the feature space. With larger training sets that may include more diverse or noisy samples, the decision boundaries can become less defined, potentially reducing generalization performance. To mitigate overfitting concerns, future implementations should consider techniques such as feature selection, dimensionality reduction, or ensemble methods. Cross-validation approaches could also provide more robust performance estimates and reduce the impact of random data splitting variations.

The KNN method is classified as a lazy learning algorithm [23] and is highly sensitive to the underlying data. When using a percentage split for evaluation, the results can vary significantly. These differences occur because the data split for training and testing changes with each iteration. The performance of KNN models stems from their dependence on data distribution characteristics; training data splits lack adequate representativeness, models may exhibit suboptimal performance on test data. Moreover, the inherent randomness in data partitioning processes, especially when training and testing sets are separated randomly without fixed seed values, introduces variations in data selection that cause evaluation results to fluctuate with each execution. This performance variability presents significant challenges, particularly with smaller datasets where the effects of data splitting fluctuations have a more pronounced impact on model reliability and consistency [24].

3.3 Clinical Implications

The developed system demonstrates potential for clinical implementation as a diagnostic support tool. The high recall rate (96%) ensures excellent sensitivity for stroke detection, minimizing falsenegative cases that could delay critical treatment. The balanced precision (91%) maintains adequate

specificity to avoid unnecessary interventions. The system's simplicity and computational efficiency make it particularly valuable in emergency settings, where rapid diagnosis is critical for achieving optimal patient outcomes.

3.4 Limitations and Future Directions

Several limitations warrant consideration. The constrained dataset size may limit generalizability, particularly for less common stroke subtypes such as lacunar infarcts or specific hemorrhagic patterns that might be underrepresented. The use of data from a single institution could introduce selection bias related to specific imaging protocols, patient demographics, or disease severity distributions. Although standardized protocols were used to minimize this concern, manual preprocessing steps may introduce operator variability. Furthermore, limited validation on external datasets restricts the assessment of the system's generalizability across different clinical settings, CT scanner manufacturers, and patient populations with varying comorbidities.

Future research directions should include validation on larger, multi-institutional datasets to assess generalizability across diverse clinical environments and imaging protocols. Integration with deep learning approaches could potentially combine the interpretability of texture features with the powerful feature-learning capabilities of neural networks. For real-time implementation in clinical workflows, the development of user-friendly interfaces and integration with existing hospital information systems will be essential. Extending the method to classify stroke subtypes could provide more detailed diagnostic information to guide specific treatment strategies. Additionally, investigating the method's performance across different stroke severity levels and time windows from symptom onset would enhance its clinical utility.

4. Conclusion

This study presents a robust texture-based classification system for automated stroke detection in CT scan images. The combination of histogram analysis, GLCM, and GLRLM features with KNN classification achieved 93% accuracy, 91% precision, and 96% recall. These results demonstrate the potential for computer-aided diagnosis systems to support clinical decision-making in acute stroke management.

The significant texture differences identified between normal and stroke images provide quantitative biomarkers that may enhance diagnostic accuracy and reduce interpretation variability. The integration of multiple texture analysis methods proved superior to single-feature approaches, with histogram features contributing significantly to classification performance through enhanced detection of tissue heterogeneity. implementation of such systems could particularly benefit emergency settings where rapid, accurate

diagnosis is critical for achieving optimal patient outcomes.

While this study demonstrates promising results, limitations—including dataset size constraints and single-source data collection, suggest the need for larger, multi-institutional validation studies. Future research should focus on real-time clinical implementation, integration with existing healthcare workflows, and extension to stroke subtype classification to maximize clinical impact. The potential clinical significance of this research lies in its ability to provide rapid, objective, and consistent diagnostic support that could reduce diagnostic delays and improve patient outcomes in acute stroke management.

Acknowledgment

The authors acknowledge Afridi Rahman, the contributor of the Brain Stroke CT Image Dataset on Kaggle, for providing the essential data used in this research. The dataset is distributed under the Creative Commons Attribution (CC BY) license, which permits use with proper attribution.

References

- [1] D. Cahyanti, A. Rahmayani, and S. A. Husniar, "Analisis Performa Metode Knn pada Dataset Pasien Pengidap Kanker Payudara" Indones. J. Data Sci., 1(2), 39–43, (2020).
- [2] I. A. Wisky and Sumijan, "Deteksi Tepi untuk Mendeteksi Kondisi Otak Menggunakan Metode Prewitt" J. Teknol., 12(2), 34–39, (2022).
- [3] P. Budianto, D. K. Mirawati, H. R. Prabaningtyas, S. E. Putra, F. Muhammad, and M. Hafizhan, Stroke Iskemik Akut Dasar dan Klinis Surakarta, (2021).
- [4] K. Anam, A. R. Chaidir, and F. Isman, "Hand Motion Strength Forecasting using Extreme Learning Machine for Post-Stroke Rehabilitation" J. Teknol. dan Sist. Komput., 9(2), 70–76, (2021).
- [5] Y. Oktarina, N. Nurhusna, K. Kamariyah, and S. Mulyani, "Edukasi Kesehatan Penyakit Stroke pada Lansia" Med. Dedication J. Pengabdi. Kpd. Masy. FKIK UNJA, 3(2), 106–109, (2021).
- [6] Sumijan, P. A. W. Purnama, and S. Arlis, "Peningkatan Kualitas Citra CT-Scan dengan Penggabungan Metode Filter Gaussian dan Filter Median" J. Teknol. Inf. dan Ilmu Komput., 6(6), 591–600, (2019).
- [7] I. Rizky, N. P. R. Jeniyanthi, and C. I. A. Widiastuti, "Prosedur Pemeriksaan CT Scan Kepala dengan Klinis Stroke Hemorrhagic di RS Bhayangkara Makassar" J. Educ. Innov. Public Heal., 2(1), 101–106, (2024).
- [8] Sukatin, Nurkhalipah, A. Kurnia, D. Ramadani, and Fatimah, "Pengaruh Variasi Rekonstruksi Slice Thickness dan Filter Kernel Terhadap Kualitas Citra CT-Scan Kepala pada Kasus Stroke Iskemik" J. Ilm. Multi Disiplin Indones., 1(9), 1278–1285, (2022).
- [9] I. W. A. W. Kusuma and A. Kusumadewi, "Penerapan Metode Contrast Stretching, Histogram Equalization dan Adaptive Histogram

- Equalization untuk Meningkatkan Kualitas Citra Medis MRI" Simetris J. Tek. Mesin, Elektro dan Ilmu Komput., 11(1), 1–10, (2020).
- [10] C. Huang and C. Chen, "Texture Analysis Based on Gray Level Co-occurrence Matrix for CT Images: A Review" Multimed. Tools Appl., (2020).
- [11] J. Sofian and R. H. Laluma, "Klasifikasi Hasil Citra Mri Otak Untuk Memprediksi Jenis Tumor Otak dengan Metode Image Threshold dan GLCM menggunakan Algoritma k-NN (Nearest Neighbor) Classifier Berbasis Web" Infotronik, 4(2), 51–56, (2019).
- [12] N. Nafisah, R. I. Adam, and C. Carudin, "Klasifikasi K-NN dalam Identifikasi Penyakit COVID-19 Menggunakan Ekstraksi Fitur GLCM" J. Appl. Informatics Comput., 5(2), 128–132, (2021).
- [13] N. Sakinah, T. Badriyah, and I. Syarif, "Analisis Kinerja Algoritma Mesin Pembelajaran Untuk Klasifikasi Penyakit Stroke Menggunakan Citra CT Scan" J. Teknol. Inf. dan Ilmu Komput., 7(4), (2020).
- [14] B. Agustina and A. R. Isnain, "Penerapan Deep Learning pada Sistem Klasifikasi Tumor Otak Berbasis Citra CT Scan" Indones. J. Comput. Sci., 13(3), 4557–4565, (2024).
- [15] M. A. Lutfia, F. X. A. Setyawan, S. Alam, T. Yulianti, and H. Fitriawan, "Implementasi Ekstraksi Fitur Menggunakan Gray Level Co-Occurrence Matrices (GLCM) dan K-Nearest Neighbor (K-NN) Untuk Klasifikasi Jenis Kain Dasar" in Seminar Nasional Teknik Elektro, 3–8, (2023).
- [16] R. Krisdiyanto and H. Sumarti, "Classification of Mammographic Image Based on Texture Features with Random Forest Method for Identification of Breast Tumors" J. Holist. Med. Technol., 1(1), 1–9, (2024).
- [17] J. F. Azzahra, H. Sumarti, and H. H. Kusuma, "Klasifikasi Kasus COVID-19 dan SARS Berbasis Ciri Tekstur Menggunakan Metode Multi-Layer Perceptron" J. Fis., 12(1), 16–27, (2022).
- [18] J. Lin and H. Irsyad, "Klasifikasi Pneumonia Pada Citra X-Rays Paru-Paru Menggunakan GLCM Dan LVQ" J. Algoritm., 1(2), 184–194, (2021).
- [19] S. Bulle, R. Nanmaran, T. Sathish, and R. Arulvel, "Analyzing the Effect of Feature Extraction Using GLRLM Method in Comparison with SIFT Method on ANN Based Cancer Classification Model" in AIP Conf. Proc., 2853(1), (2024).
- [20] J. Vymazal, A. M. Rulseh, J. Keller, and L. Janouskova, "Comparison of CT and MR Imaging in Ischemic Stroke" Insights Imaging, 3(6), 619–627, (2012).
- [21] N. Jannata, F. Yanto, L. Handayani, and E. P. C. Kurnia, "Pengaruh Contrast Limited Adaptive Histogram Equlization dalam Klasifikasi CT-Scan Tumor Ginjal menggunakan Deep Learning" INOVTEK Polbeng - Seri Inform., 9(1), 420–433, (2024).
- [22] F. Risal, E. Setyawan, and L. R. Rere, "Convolutional Neural Network Untuk Deteksi Covid-19 Melalui Citra Chest X-Ray" in Prosiding Seminar SeNTIK, 5(1), (2021).
- [23] A. P. Sidik, Hermansyah, and D. Aulia, "Rancangan Sistem Pengelompokkan Buah

- Berdasarkan Kadar Vitamin Menggunakan Metode K-Medoids" Perlindungan Huk. Terhadap Sertifikasi Haalal Dengan Model Self Declar., 4, 125–133, (2023).
- [24] M. Bansal, A. Goyal, and A. Choudhary, "A Comparative Analysis of K-Nearest Neighbor, Genetic, Support Vector Machine, Decision Tree, and Long Short Term Memory Algorithms in Machine Learning" Decis. Anal. J., 3, 100071, (2022).